Integrated reduction/oxidation reactions and sorption processes for Cr(VI) removal from aqueous solutions using *Laminaria digitata* macro-algae

CrossMark

Ingrid M. Dittert [a,b], Heloisa de Lima Brandão [a,b], Frederico Pina [b], Eduardo A.B. da Silva [a], Selene M.A. Guelli U. de Souza [b,*], Antônio Augusto U. de Souza [b], Cidália M.S. Botelho [a], Rui A.R. Boaventura [a], Vítor J.P. Vilar [a,*]

[a] *LSRE – Laboratory of Separation and Reaction Engineering – Associate Laboratory LSRE/LCM, Faculdade de Engenharia, Universidade do Porto, Rua Dr. Roberto Frias, 4200-465 Porto, Portugal*
[b] *Laboratório de Transferência de Massa, Departamento de Engenharia Química e Engenharia de Alimentos, Universidade Federal de Santa Catarina, PO Box 476, CEP 88040-900 Florianópolis, SC, Brazil*

HIGHLIGHTS

- Integrated reduction reactions and sorption processes for Cr(VI) removal.
- Cr(VI) is reduced to Cr(III) by contact with electron-donor groups of biomass.
- The reduced Cr(III) remains in the aqueous phase or bound to the biomass.
- The oxidized biomass presents a higher number of carboxylic groups.
- Solution pH enhances the reduction reaction but inhibits the adsorption process.

GRAPHICAL ABSTRACT
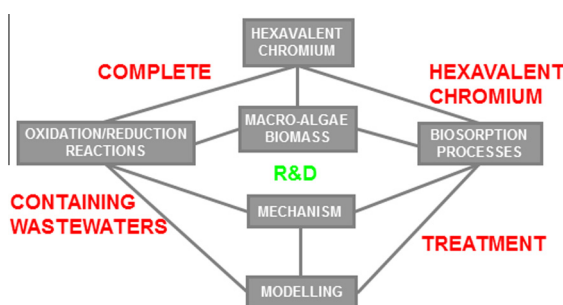
ABSTRACT

The main goal of this work was the valorization of seaweed *Laminaria digitata*, after acid pre-treatment, for the remediation of hexavalent chromium solutions. The Cr(VI) removal efficiency by the protonated bio-mass was studied as a function of different parameters, such as contact time, pH, biomass and Cr(VI) concentration, and temperature. Cr(VI) removal is based on a complex mechanism that includes a reduction of Cr(VI) to Cr(III), through the oxidation of biomass at acidic medium, and further chemical binding of Cr(III) to the negatively charged binding groups, mainly carboxylic groups. The optimum pH for chromium removal, using protonated *L. digitata* algae, was 2.5. The maximum amount of Cr(VI) reduction by the algae was around 2.1 mmol/g. The uptake capacity of Cr(III) by the oxidized biomass, after Cr(VI) reduction, was higher than by the algae in its original form (protonated algae). Results suggest that the oxidation of the biomass during Cr(VI) reduction, turns other active sites available for Cr(III) binding. Also, the Cr(III) binding from a solution of reduced Cr(VI) was much lower than from a pure Cr(III) solution. The result suggests the presence in solution of Cr(III) complexes with the organic matter released from the algae surface during Cr(VI) reduction. The activation energy obtained for the Cr(VI) reduction by *L. digitata* was 45 ± 20 kJ mol^{-1}. A kinetic model based on the redox reaction between Cr(VI) species and organic compounds from the biosorbent surface was able to fit well the hexavalent chromium concentration. Trivalent chromium equilibrium biosorption was well described at different chromium concentrations, considering the interaction between carboxylic groups present in the surface of the biomass and Cr(III) in solution.

© 2013 Elsevier B.V. All rights reserved.

* Corresponding authors. Tel.: +55 (48) 3721 9448; fax: +55 (48) 3721 9687 (S.M.A.G.U. de Souza), tel.: +351 918257824; fax: +351 225081674 (V.J.P. Vilar).
E-mail addresses: selene@enq.ufsc.br (S.M.A.G.U. de Souza), vilar@fe.up.pt (V.J.P. Vilar).

Nomenclature

A	Arrhenius's frequency factor	K'_H	average of the affinity distribution of hydrogen ions
B	biomass	$K_{i,H}^{int}$	intrinsic proton affinity constant at each binding site i
B_T or Q_{max}	total number of binding sites B per unit mass of biomass (mmol g^{-1})	K_H	dissociation constant of functional group (mol L^{-1})
C_H	proton concentration in the solution (mmol L^{-1})	m_H	width of the Sips distribution
C_{OC}^*	content of organic compound equivalent per unit gram of biomaterial (mmol g^{-1})	n	order of reaction with respect to proton concentration
$[OC]_0$	initial concentration of organic compound (mmol g^{-1})	Q_H	weighted sum of the charge contributions of each active site (mmol g^{-1})
E_a	activation energy (J mol^{-1})	R	gas constant (8.314 J mol^{-1} K^{-1})
f	oxidation factor	t	time (s)
F_{obj-a}	objective function	T	solution temperature (K)
i	experimental sample number	X_{OXI}	fraction of organic compound oxidized
k	kinetic rate coefficient of hexavalent chromium reduction (L mmol^{-1} s^{-1})	$\theta_{T,H}$	total degree of protonation

1. Introduction

Chromium can exist in eleven valence states ranging from –IV to +VI, however, only Cr(III) and Cr(VI) are sufficiently stable to occur in the natural environment [1]. Cr(III) is usually found bound to organic matter in soil and in aquatic environments and Cr(VI) is usually associate with oxygen, such as oxyanions chromate (CrO_4^{2-}) and dichromate ($Cr_2O_7^{2-}$) [2]. These two divalent oxyanions are very water soluble and poorly adsorbed by soil and organic matter, making them mobile in soil and groundwater. Both chromate anions represent acute and chronic risks to animals and human health, since they are extremely toxic, mutagenic, carcinogenic, and teratogenic [3]. Cr(VI) oxyanions are readily reduced to trivalent forms, which are comparatively less toxic, when they come into contact with electron donors that are present in organic matter, or with reduced inorganic species present in soil, water and the atmosphere [4]. Most of the Cr(VI) found in the nature is the result of domestic and industrial emissions [5]. The nature and behavior of the various forms of chromium found in natural waters can be quite different from those found in wastewater, due to the variety of physical–chemical natures of the effluents discharged from various industrial sources. The presence and concentration of chromium in wastewaters is mainly dependent on the form of the chromium applied in industrial processes, the pH and the amount of organic and/or inorganic residues. Cr(VI) is present predominantly in wastewater effluents from heavy industrial processes, such as those derived from the metallurgical, metal finishing (hard chromium plating) and refractory industries and from the production and application of pigments (chromate color and corrosion inhibitors pigments) [4]. Chemical methods can be used for the treatment of Cr(VI) containing wastewaters, involving aqueous reduction of Cr(VI) to Cr(III), at acidic pH values, using various chemical reagents with subsequent pH adjustment (neutral pH values) leading to Cr(III) precipitation. However, these methods are considered undesirable due to the use of expensive and toxic reagents, low removal efficiency for low chromium concentrations and the production of large amounts of chemical waste [6]. Wastewaters that contains relatively low Cr(VI) concentrations are usually treated with ion exchange resins. This procedure offers the advantage of recovering chromic acid, however, it is an expensive technique due to the high cost of the resin [7]. In this scenario, the biosorption process, using low cost materials, appears to be a highly effective and economical alternative for the removal of Cr(VI) from wastewater [8]. It has been reported that Cr(VI) can be reduced to Cr(III) in aqueous solutions using different solid biomaterials, especially at acidic conditions [9–12]. Gardea-Torresdey

et al. [13] reported that Cr(VI) was easily reduced to Cr(III) using oat processing byproduct, and subsequently adsorbed by the available negatively charged carboxylic groups. During Cr(VI) reduction, a fraction of the organic carbon from the biosorbent, was completely oxidized into inorganic carbon, in the form of HCO_3^- and CO_2. The oxidation of the biomass supplies the electrons necessary for the Cr(VI) reduction reaction. For the Cr(VI) reduction to Cr(III), not only electrons, but also protons are necessary, meaning that the reaction rate depends on the solution pH, decreasing with the increment of pH. Sawalha et al. [14] studied the effect of pH on chromium binding employing native, esterified, and hydrolyzed saltbush (*Atriplex canescens*) biomass. X-ray absorption spectroscopy results showed that Cr(VI) was reduced in some extent to Cr(III) by the saltbush biomass at both pH 2.0 and pH 5.0. Park et al. [15] reported the removal of Cr(VI) employing sixteen biomaterials and using XPS analysis to verify the oxidation state of the Cr bound to the biomaterials. Although, the chromium bound to the surface of these biomaterials was mostly or totally in the trivalent form in the final pH range of 2.17–2.50, the reduction reaction of Cr(VI) to Cr(III) also occurred on the surface of the biomaterials.

Laminaria digitata is a large brown algae, found normally at the sub littoral zone of the northern Atlantic Ocean, reaching up to 4 m length, which was traditionally used as fertilizer and for the extraction of iodine [16]. Nowadays it has been used for the extraction of alginic acid, the manufacture of toothpastes and cosmetics, and in the food industry for binding, thickening and moulding [17,18]. In Portugal, big amounts of *L. digitata* can be found in the beaches, threaten the tourist industry by spoiling pristine environments. Turning macro-algae *L. digitata* into a resource for biosorption processes can be quite beneficial to some local economies.

The main objective of this work was to study the mechanism of hexavalent chromium removal in aqueous solutions using brown macro-algae *L. digitata*. The efficiency of the process was evaluated at different operational conditions, such as hexavalent chromium concentration, solution pH and temperature and biomass concentration. A kinetic model based on integrated reduction/oxidation reactions and sorption processes on the surface of the biomass was used to describe the behavior of hexavalent, trivalent and total chromium concentration in the aqueous and solid phase.

2. Mathematical models

2.1. Quantification of functional groups

Since the algal surface is polyfunctional, each site of each functional group reacts with protons with different affinities. The

distribution of affinity defines the chemical heterogeneity of the active sites present at the surface of the biomass. The total degree of protonation, $\theta_{T,H}$, can be obtained from the Langmuir–Freundlich isotherms. Assuming a quasi-Gaussian distribution, the affinity constant suggested by Sips [19] can be described by Eq. (1):

$$\theta_{T,H} = \frac{(K'_H C_H)^{m_H}}{1 + (K'_H C_H)^{m_H}} \tag{1}$$

where K'_H is the average of the affinity distribution of hydrogen ions, which determines the position of the affinity distributions along the axis $\log K^{int}_{i,H}$ ($K^{int}_{i,H}$ is the intrinsic proton affinity constant at each binding site i), C_H is the proton concentration in the solution and m_H is related to the width of the Sips distribution, which can have values between 0 and 1, representing an infinite width and a null width, respectively. It should be noted that the parameter m_H is a measure of the overall heterogeneity, which includes the chemical heterogeneity. If the distribution of affinity displays more than one peak, then the charge of the acid surface, Q_H, is expressed as a weighted sum of the charge contributions of each active site:

$$Q_H = \sum_j Q_{max,j}(1 - (\theta_{T,H})_j) \tag{2}$$

Assuming the presence of two different types of ligands, carboxyl ($j = 1$) and hydroxyl ($j = 2$), the equation of the continuous model [20,21] is obtained:

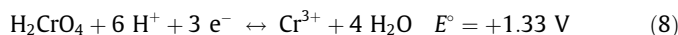$$Q_H = \frac{Q_{max,1}}{1 + (K'_{1,H} C_H)^{m_{H,1}}} + \frac{Q_{max,2}}{1 + (K'_{2,H} C_H)^{m_{H,2}}} \tag{3}$$
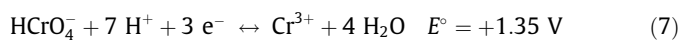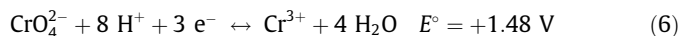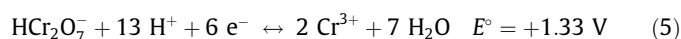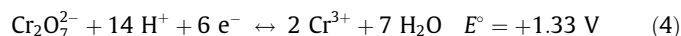
where $Q_{max,1}$ and $Q_{max,2}$ are the maximum concentrations of carboxyl and hydroxyl groups, respectively.

The mathematical model was fitted to the experimental data using the Excel Solver (Quasi-Newton algorithm). In order to determine the errors associated with the parameters ($K'_{1,H}$, $K'_{2,H}$, $Q_{max,1}$, $Q_{max,2}$, $m_{H,1}$, $m_{H,2}$), the matrix inversion approach [22] was used.

2.2. Kinetic modeling of Cr(VI) reduction

A good knowledge of hexavalent chromium speciation in solution is necessary to understand the chromium removal by integrated oxidation/reduction reactions and sorption processes. Cr(VI) exists in different ionic forms (H_2CrO_4, $HCrO_4^-$, CrO_4^{2-}, $Cr_2O_7^{2-}$ and $HCr_2O_7^-$), depending on the solution pH and chromium concentration. Considering the pH working range and chromium concentration used in this work, two Cr(VI) speciation diagrams were constructed (Fig. A – Supplementary data file), for Cr(VI) concentrations of 0.2 mM and 6.0 mM ($T = 25$ °C; Ionic strength = 0 M) [23]. For the lowest chromium concentration (0.2 mM), and $1.0 < $ pH $ < 4.0$, $HCrO_4^-$ anion is the predominant species, with a molar fraction above 92% ($0 < [H_2CrO_4] < 7.6\%$). However, for higher total Cr(VI) concentrations, the molar fraction of $HCrO_4^-$ anion decreases and the molar fraction of $Cr_2O_7^{2-}$ anion increases. For a total Cr(VI) concentration of 6 mM, in the range of working pHs values (1–4) used in this work, the molar fractions for $HCrO_4^-$, and $Cr_2O_7^{2-}$ anions are between 79–85% and 13–15%, respectively ($0 < [H_2CrO_4] < 6.5\%$).

Hexavalent chromium species are also strong oxidants, which have the tendency to be reduced to trivalent chromium species, according to the following reactions ($E°$-standard potentials; $T = 25$ °C) [24], which is greatly influenced by the solution pH.

$$Cr_2O_7^{2-} + 14 \ H^+ + 6 \ e^- \leftrightarrow 2 \ Cr^{3+} + 7 \ H_2O \quad E° = +1.33 \ V \tag{4}$$

$$HCr_2O_7^- + 13 \ H^+ + 6 \ e^- \leftrightarrow 2 \ Cr^{3+} + 7 \ H_2O \quad E° = +1.33 \ V \tag{5}$$

$$CrO_4^{2-} + 8 \ H^+ + 3 \ e^- \leftrightarrow Cr^{3+} + 4 \ H_2O \quad E° = +1.48 \ V \tag{6}$$

$$HCrO_4^- + 7 \ H^+ + 3 \ e^- \leftrightarrow Cr^{3+} + 4 \ H_2O \quad E° = +1.35 \ V \tag{7}$$

$$H_2CrO_4 + 6 \ H^+ + 3 \ e^- \leftrightarrow Cr^{3+} + 4 \ H_2O \quad E° = +1.33 \ V \tag{8}$$

Depending on the type of hexavalent chromium species present in solution, different number of electrons and protons are requested to achieve total reduction to trivalent chromium. Increasing the total chromium concentration, the molar fraction of $Cr_2O_7^{2-}$ species increases, leading to a substantially increment in the number of electrons and protons necessary for the reduction process.

Park et al. [25–29] proposed a direct and/or indirect mechanism for Cr(VI) elimination by seaweed and fungal biomasses: (a) direct reduction mechanism, by which Cr(VI) is directly reduced to Cr(III) in the aqueous phase by contact with electron–donor groups of the biomass, and the reduced Cr(III) remains in the aqueous phase or bound to the negatively charged groups; and (b) indirect reduction mechanism that consists of three steps: (i) the binding of anionic Cr(VI) species to positively-charged groups present on the surface of the biomass, (ii) the reduction of Cr(VI) into Cr(III) by adjacent electron-donor groups and (iii) the release of Cr(III)-reduced ions into aqueous phase due to electrostatic repulsion between positively-charged groups and Cr(III), or the reduced-Cr(III) complexation with adjacent negatively charged groups.

Considering that *L. digitata* presents mainly carboxylic (alginic acid) and sulfonic groups (fucoidan) [17,30], the binding of anionic Cr(VI) can be only possible at very low pH values, where the functional groups are completely protonated and can be positively charged. Low pH values increase the reduction reaction since the attraction of Cr(VI) species to the surface of the biomass is enhanced and protons are also available for the reduction reaction. Biomaterials are also electron-donors, mainly due to the oxidation of thiol and phenolic groups, as reported by several authors [31,32]. The cationic Cr(III) ions in the aqueous phase can bind to the negatively charged carboxylic and sulfonic groups. Low pH values favors the Cr(VI) reduction kinetics but decreases the total chromium removal, since functional groups are protonated or positively charged and protons compete with Cr(III) ions to the same binding sites.

Considering the aspects reported above, a kinetic model, as proposed by Park et al. [33,34], for the Cr(VI) reduction using biomaterials, was used to describe the Cr(VI) removal by *L. digitata* seaweed based on the redox reaction between Cr(VI) and the biomaterial:

$$Biomass + Cr(VI) \xrightarrow{k} Biomass \ (oxidized) + Cr(III) \tag{9}$$
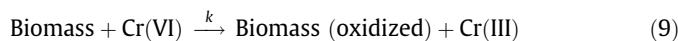
The following assumptions are considered: (i) organic compounds in the biosorbent are responsible for reducing Cr(VI), (ii) only one kind of organic compound (OC) is capable of reducing Cr(VI), (iii) the equation rate for the Cr(VI) reduction is first-order (Eq. (9)) with respect to both the Cr(VI) concentration and the concentration of OC capable of reducing Cr(VI), (iv) no significant biomass loss during the oxidation process and (v) 1:1 stoichiometric ratio between Cr(VI) and Cr(III), considering that the predominant hexavalent chromium species in solution are hydrogen chromate ($HCrO_4^-$) and chromic acid (H_2CrO_4) ($Cr_2O_7^{2-}$ is below 15%). When the pH and temperature are constant the rate of Cr(VI) reduction by an organic compound can be found as:

$$\frac{d[Cr(VI)]}{dt} = -k[OC][Cr(VI)] \tag{10}$$

where [OC] represents the equivalent organic compound concentration at time t capable of reducing Cr(VI) (mmol L^{-1}), [Cr(VI)] is the hexavalent chromium concentration (mmol L^{-1}) at time t and k its rate coefficient (L mmol^{-1} s^{-1}).

Considering that electron–donors groups are oxidized during Cr(VI) reduction, which was confirmed by the release of organic carbon during the oxidation process (increment of dissolved organic carbon in solution), the equivalent organic compound concentration in the surface of the biomass decreases during the reaction and can be calculated as:

$$[OC]_t = C_{OC}^*[B]\left(1 - \frac{[Cr(VI)]_0 - [Cr(VI)]_t}{C_{OC}^*[B]}\right) \qquad (11)$$

where [B] is the biomaterial concentration (g L^{-1}), [Cr(VI)]$_0$ is the initial hexavalent chromium concentration (mmol L^{-1}), C_{OC}^* is the concentration of equivalent organic compound per unit gram of biomaterial (mmol g^{-1}), i.e., the C_{OC}^* value for *Laminaria* is 2.1 mmol g^{-1}, obtained by the biomass limited experiment. The product, $C_{OC}^*[B]$, represents the initial concentration of OC and $([Cr(VI)]_0 - [Cr(VI)]_t)/(C_{OC}^*[B])$ represents the fraction of OC oxidized (X_{OXI}).

Substituting Eqs. (11) in (10), and integrating, results in:

$$[Cr(VI)]_t = \frac{C_{OC}^*[B][Cr(VI)]_0 - [Cr(VI)]_0^2}{C_{OC}^*[B]\exp\{k(C_{OC}^*[B] - [Cr(VI)]_0)t\} - [Cr(VI)]_0} \qquad (12)$$
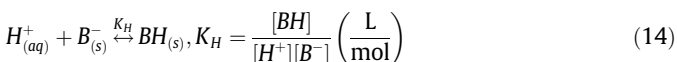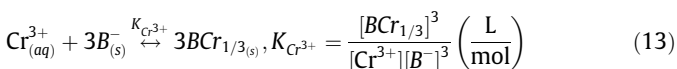
where k and C_{OC}^* are the model constant parameters and t is the variable time (s).

The mathematical model was fitted to the experimental data obtained from kinetic studies using the Excel Solver (Quasi-Newton algorithm). The errors associated with the parameters were determined using the matrix inversion approach [22].

2.3. Cr(III) biosorption

2.3.1. Equilibrium

In aqueous solutions, within the pH range used in this work (<4), Cr^{3+} and CrOH^{2+} are the most abundant species, present in equal amounts at pH 3.55 [35]. In addition, the biosorption of trivalent chromium is qualitatively shown to involve a process of cationic exchange between chromium ions (Cr^{3+} and/or CrOH^{2+}) and the protons of the carboxylic groups of the biomass [36]. The biosorption of metal cations can be explained by the complexation with the negative charged groups present in the surface of the biomass. Considering the monovalent carboxylic groups (B) responsible for chromium binding, and initially saturated with hydrogen ions, and for a pH value of 2.5, optimum pH for total chromium removal, Cr^{3+} represents 92% of the total trivalent chromium species [37], the binary complexation system can be described by the following reactions:

$$Cr_{(aq)}^{3+} + 3B_{(s)}^- \overset{K_{Cr^{3+}}}{\leftrightarrow} 3BCr_{1/3(s)}, K_{Cr^{3+}} = \frac{[BCr_{1/3}]^3}{[Cr^{3+}][B^-]^3}\left(\frac{L}{mol}\right) \qquad (13)$$

$$H_{(aq)}^+ + B_{(s)}^- \overset{K_H}{\leftrightarrow} BH_{(s)}, K_H = \frac{[BH]}{[H^+][B^-]}\left(\frac{L}{mol}\right) \qquad (14)$$

where K_H and $K_{Cr^{3+}}$ are the equilibrium binding constants of H$^+$ and Cr^{3+} to the binding site (L mol^{-1}), respectively, [H$^+$] and [Cr^{3+}] are the equilibrium concentrations of H$^+$ and Cr^{3+} in the liquid phase, [B$^-$] the number of free binding sites per unit mass of biomass (mmol g^{-1}), [BH] and [BCr$_{1/3}$] are the equilibrium concentrations of H$^+$ and Cr^{3+} in the solid phase (mmol g^{-1}), respectively.

Here, the metal–ligand binding sites were considered as $BCr_{1/3}$ instead of B_3Cr, respectively, to emphasize that three bonds have to be broken in competitive binding or upon desorption of the metal, as formulated by [38].

When the biomass reacts with the metal in solution, the ligand sites become occupied by Cr^{3+} and H$^+$ or remain free. Therefore, the mass balance for the sites can be described as:

$$[B]_T = [B^-] + [BH] + [BCr_{1/3}] \qquad (15)$$

where $[B]_T$ is the total number of binding sites B per unit mass of biomass (mmol g^{-1}). Substituting Eqs. (13) and (14) in (15), the concentration of free sites can be expressed as:

$$[B^-] = \frac{[B]_T}{1 + K_H[H^+] + \sqrt{K_{Cr^{3+}}[Cr^{3+}]}} \qquad (16)$$

The amount of chromium adsorbed ($q_{Cr^{3+}} = [BCr_{1/3}]/3$) can be calculated combining Eqs. (13) and (16), which gives:

$$q_{Cr^{3+}} = \frac{([B]_T/3)\sqrt[3]{K_{Cr^{3+}}[Cr^{3+}]}}{1 + K_H[H^+] + \sqrt[3]{K_{Cr^{3+}}[Cr^{3+}]}} \qquad (17)$$

Considering that during the hexavalent chromium reduction, and consequently oxidation of the biomass, the number of negatively groups available for the trivalent chromium binding increases, Eq. (17) was rewritten as follows:

$$q_{Cr^{3+}} = \frac{\{[B]_T(1 + fX_{OXI})/3\}\sqrt[3]{K_{Cr^{3+}}[Cr^{3+}]}}{1 + K_H[H^+] + \sqrt[3]{K_{Cr^{3+}}[Cr^{3+}]}} \qquad (18)$$

where $[B]_T \times f \times X_{OXI}$ represents the fraction of sites generated during the biomass oxidation. The experimental data obtained from equilibrium studies were fitted to the mathematical model using the Excel Solver (Quasi-Newton algorithm). In order to determine the errors associated with the parameters, the matrix inverse approach [22] has been used.

2.3.2. Kinetics

In order to determine the trivalent chromium concentration in the liquid and solid phase at a certain time, a mass balance to the total chromium can be made, since the sum of chromium present in aqueous solution and on the biomass is always constant:

$$[Cr(VI)]_0 = [Cr(VI)]_t + [Cr(III)]_t + q_{Cr^{3+}}[B] \qquad (19)$$

Considering that the limit step of the integrated process is the hexavalent chromium reduction, and trivalent chromium sorption is instantaneous at the surface of the biomass (reduced Cr(III) remains in equilibrium state between the biomass and aqueous solution), for a certain time, the trivalent chromium concentration present in the aqueous solution, [Cr(III)]$_t$, can be obtained solving the mass balance combining Eqs. (12), (18), and (19). The amount of trivalent chromium in the solid phase can be calculated by substituting the trivalent chromium concentration at each time, [Cr(III)]$_t$, in Eq. (18).

3. Material and methods

3.1. Biosorbent preparation

L. digitata seaweed biomass was collected at the Northern coast of Portugal, washed with tap water, sun-dried and cut into pieces of 0.5–1 cm length. The protonated biomass was prepared by washing 10 g L^{-1} of biomass with 0.2 M HNO$_3$ in 2 cycles of 3 h each. The acid treatment is necessary to convert the insoluble alginate salts present in the cell walls into alginic acid [18]. This procedure was carried out using a 5-L capacity glass vessel and a mechanical shaker (VWR VOS 14) provided with a Teflon paddle.

The acid treated biomass was washed several times with distilled water until it reached pH 4.0 and then dried in an oven (Binder, WT) at 45 °C for 24 h. The material treated with the acid solution is referred to herein as the protonated algae.

3.2. Reactants

The chromium solutions were prepared from the salt K_2CrO_4 (Fluka). Solutions of diphenylcarbazide (Merck), NaOH and HNO_3 were also used.

3.3. Analytical determinations

The total chromium concentration in aqueous solution was determined by atomic absorption spectrometry (AAS, GBC 932 Plus) with a nitrous oxide-acetylene flame, a spectral slit width of 0.2 nm, and working current/wavelength of 6.0 mA/357.9 nm, giving a detection limit of 0.08 mg L^{-1}. The hexavalent chromium concentration was measured by molecular absorption spectrophotometry (UNICAM – HEλIOS spectrophotometer). The procedure followed is based on the formation of a pink complex of Cr (VI) with 1,5-diphenylcarbazide in acid solution which absorbs at 540 nm [39]. The trivalent chromium was determined by the difference between the measurements of total and hexavalent chromium.

Dissolved organic carbon (DOC) content was determined in a TC-TOC-TN analyzer equipped with an ASI-V autosampler (Shimadzu, model TOC-V_{CSN}) and provided with a NDIR detector, calibrated with standard solutions of potassium hydrogen phthalate (total carbon) and a mixture of sodium hydrogen carbonate/carbonate (inorganic carbon). The total organic carbon of the solid samples was obtained using the same TC-TOC-TN analyzer coupled with a solid sample combustion unit (SSM-5000A).

To determine the amount of chromium present in the protonated and chromium loaded biomass, the samples were digested at 140 °C during 2 h (G. Vittadini RECOD/6 Test), adding 5 mL distilled water, 12 mL HCl (37%) and 4 mL HNO_3 (65%) to 0.5 g of sample. After cooling, the metal concentration in the solution was determined by AAS after filtration through cellulose acetate membrane filters (Ref. Albet-CA-045-25-BI).

3.4. Fourier transform infrared (FTIR) analysis

The identification of the functional groups on the surface of the biosorbent was performed by infrared spectroscopy. The algal samples were ground and dried at 45 °C for 24 h and analyzed by infrared spectrometry (Shimadzu FTIR IRAffinity with an EasiDiff diffuse reflectance accessory, Pike Technologies) in the solid form. Spectra were registered from 4000 to 400 cm^{-1}.

3.5. Potentiometric titration

The potentiometric titration was performed using an automatic titration system (Metrohm, 702 SM Titrino) and a shaker module (Metrohm, 728 stirrer). The pH electrode was calibrated with buffer solutions of pH 1.00, 4.01, 7.00 and 9.00. For each titration, 0.25 g of protonated algal biomass was added to 50 mL of a 0.1 mol L^{-1} NaCl solution and this suspension was then placed in a titration thermostatic cell at 25 °C. First of all, the suspension was acidified to pH 2.4–2.6 by adding a specific volume of 0.1 mol L^{-1} HCl solution and bubbled for 30 min with nitrogen gas to remove dissolved CO_2 from the solution. Afterwards, the titration was performed with stepwise addition of 0.02 mL of a 0.1 mol L^{-1} NaOH solution (Titrisol, Merck) to the cell until pH 10, while the suspension was stirred under nitrogen atmosphere. When the drift between each addition was less than

0.5 mV min^{-1} or there was a 30 min break between each NaOH addition, it was considered that equilibrium had been reached. The data on the base volume added and the pH were continuously recorded.

3.6. Cr(VI) reduction kinetics

Cr(VI) reduction kinetic study was conducted in a 1000 mL glass reactor containing 800 mL of the metal solution, equipped with a cooling jacket to ensure a constant temperature during the experiments. Experiments were done at different solution pH (1.0, 1.5, 2.0, 2.5, 3.0, 3.5 and 4.0; [Cr(VI)] = 0.2 mM; 4 g biomass L^{-1}; T = 20 °C), different initial Cr(VI) concentrations (0.2; 1.1 and 6.2 mM; pH = 2.5; 4 g biomass L^{-1}; T = 20 °C), different biomass concentrations (0.5, 1.0, 2.0, 4.0 and 6.0 g L^{-1}; [Cr(VI)] = 0.2 mM; pH = 2.5; T = 20 °C), and different temperatures (10, 20, 30 and 40 °C; [Cr(VI)] = 0.2 mM; pH = 2.5; 4 g biomass L^{-1}). The suspensions were mechanically stirred at 150 rpm (VWR VOS). The pH was adjusted using HNO_3 solution since there was an increase in pH. The mass balance to the protons concentration includes: (i) proton consumption during the Cr(VI) reduction, according to reactions 5–9; (ii) proton release from biomass during Cr(III) binding via proton–Cr(III) ion exchange (since the biomass used has been protonated initially, the negatively charged groups responsible by Cr(III) binding are initially protonated); (iii) consumption of protons for the chromium hydrolysis reaction; and (iv) protonation of the binding sites generated during the biomass oxidation. Samples were collected at predetermined time intervals and filtered through cellulose acetate membrane filters (Sartorius Stedim).

To quantify the maximum Cr(VI) reducing capacity of L. digitata, a high concentration of Cr(VI), 4.1 mM, was put into contact with a small amount (1.0 g/L) of biomass (biomass limiting experiment) under acid conditions (pH = 2.5) and T = 20 °C. The suspension was maintained under constant agitation of 150 rpm in a shaker (VWR Advanced Digital Shaker) during 4 weeks, until achieve a constant Cr(VI) concentration, different from zero. To evaluated the influence of the presence of Cr(III) in Cr(VI) reduction kinetics, experiments with a solution of 1.8 mM of Cr(VI) concentration without and with 4.8 mM of Cr(III) concentration were performed (conditions: V = 250 mL, pH 2.5 and biomass concentration of 4 g L^{-1}). To obtain a Cr(III) solution coming from the reduction process, a Cr(VI) reduction kinetic at high concentration (6.2 mM) was carried out until total Cr(VI) reduction. The obtained Cr(III) solution with 1.2 mM was used for the adsorption kinetic at pH 4.0 using 2.0 g L^{-1} of fresh protonated biomass.

4. Results and discussion

4.1. FTIR analysis

The FTIR spectra for the protonated biomass before and after oxidation in the presence of hexavalent chromium solution ([Cr(VI)]$_0$ = 6.2 mM, [B] = 4 g L^{-1}, contact time = 143 h, pH = 2.5, X_{OXI} = 0.74; [Cr(VI)]$_0$ = 5.3 mM, [B] = 4 g L^{-1}, contact time = 47 h, pH = 1.0, X_{OXI} = 0.63) and, trivalent chromium loaded biomass ([Cr(III)]$_0$ = 1.2 mM, [B] = 2 g L^{-1}, contact time = 120 h, pH = 4.0, ($q_{Cr^{3+}}$ = 0.4 mmol g^{-1}), using the chromium solution after complete reduction of Cr(VI) to Cr(III) and protonated biomass without suffering any oxidation in a Cr(VI) solution, were used to determine the vibration frequency changes in the functional groups of the biosorbent (Fig. 1).

The region of 3400 cm^{-1} can be related to O—H and N—H stretching indicating the presence of hydroxyl and amino groups [40]. The peak at 2929 cm^{-1} represents the C—H stretching.

Changes in the peaks of the spectra are visible at wavenumbers below 1740 cm^{-1} (Fig. 1b). The peak at 1740 cm^{-1} decreases considerably for the biomass after Cr(VI) reduction at pH 2.5 and disappears for the Cr(III) loaded biomass. This suggests that there is interaction between Cr(III) produced from the reduction of Cr(VI) and the group which adsorbs in this region, i.e., carboxyl group [41]. For the reduction experiment at pH = 1, the amount of Cr(III) sorbed in the carboxyl group is low and no modification in the FTIR spectra is observed. The peak at 1532 cm^{-1}, attributed to N-H groups [40], is suppressed for the biomass after Cr(VI) reduction at pH 2.5 and Cr(III) loaded biomass, indicating interaction of the metal with this group. The peak at around 1440 cm^{-1}, attributed to C=O symmetric stretching [41], is shifter to a shorter wavelength, for the Cr(III) loaded algae. Cr(VI) is a powerful oxidizing agent, which can oxidize primary and secondary alcohols to the corresponding ketones, and carboxylic acids and other compounds with "benzyl" hydrogen to benzoic acids, while Cr(VI) is reduced to Cr(III) [32]. For the reduction at pH 1.0 there is an increase in the peak at 1743 cm^{-1}. The biomass after Cr(VI) reduction was dried and it was observed a decolorization resulting from the biomass oxidation. This indicates that the algae pigments are the main electron-donors groups responsible by the reduction of hexavalent to trivalent chromium.

4.2. Potentiometric titration

To examine the number of negatively functional groups responsible for trivalent chromium binding, a potentiometric titration of the protonated biomass before and after oxidation in the presence of an hexavalent chromium solution ([Cr(VI)]$_0$ = 6.2 mM, [B] = 4 g L^{-1}, contact time = 143 h, pH = 2.5, X_{OXI} = 0.74, $q_{Cr^{3+}}$ = 1.2 mmol g^{-1}) was performed (Fig. 2). Fig. 2 shows that the continuous model fits well the experimental data, where two peaks can be observed, and according to the $pK'_{i,H}$ values can be associated to carboxylic and hydroxyl groups [36]. Fig. 2 also shows the distribution function $F = \sum_i f_i(\log K_{i,H}^{int}) Q_{max,i}$ versus $\log K_{i,H}^{int}$ where $f_i(\log K_{i,H}^{int})$ represents the Sips distribution function for the carboxylic and hydroxyl groups with total charges $Q_{max,1}$ and $Q_{max,2}$, respectively [36]. Alginate, mannitol, laminaram and cellulose are the main constituents of the cell wall of brown seaweed *Laminaria*, which contains many carboxyl and hydroxyl groups [42].

Table 1 shows that for *L. digitata* the carboxylic groups are more abundant than the hydroxyl ones ($Q_{max,1}$ = 2.06 ± 0.01 mmol g^{-1} and $Q_{max,2}$ = 1.4 ± 0.7 mmol g^{-1}, respectively). Through the heterogeneity distribution parameter $m_{H,i}$, low $m_{H,i}$ values correspond to a wider distribution and also a greater heterogeneity of the groups, it can be observed that the hydroxyl groups are more heterogeneous than carboxylic groups. A high increase of carboxylic groups (0.91 mmol g^{-1}) was obtained for the oxidized biomass after Cr(VI) reduction. Considering that the amount of trivalent chromium sorbed on the oxidized biomass, $q_{Cr^{3+}}$, is 1.2 mmol g^{-1} (assuming as negligible the loss of biomass during the biomass oxidation), the number of carboxylic groups generated during the oxidation process is ~4.5 mmol per gram of biomass (total binding groups of 6.57 mmol g^{-1} for X_{OXI} = 0.74, assuming that each mmol of Cr^{3+} occupies three mmol of carboxylic groups). Similar results were obtained by Dupont and Guillon [31] who studied the removal of Cr(VI) by a lignocellulosic substrate extracted from wheat bran. They reported that the oxidation of lignin moieties occurred concomitantly with the Cr(VI) reduction and led to the formation of carboxyl and hydroxyl groups.
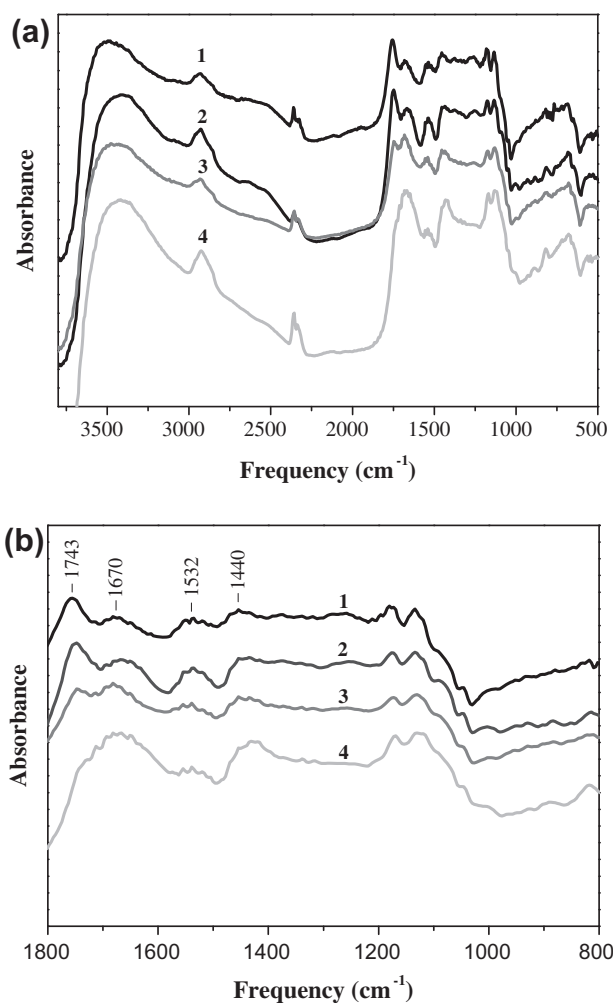

Fig. 1. (a) Fourier transform infrared spectra of different algae samples; (b) high resolution graph: 1 – protonated biomass, 2 – protonated biomass after Cr(VI) reduction at pH 1.0 (X_{OXI} = 0.63; [Cr(VI)]$_0$ = 5.3 mM; [Cr(VI)]$_{final}$ = 0.003 mM; $q_{Cr^{3+}}$ = 0.14 mmol g^{-1}; 3 – protonated biomass after Cr(VI) reduction at pH 2.5 (X_{OXI} = 0.74; [Cr(VI)]$_0$ = 6.2 mM; [Cr(VI)]$_{final}$ = 0.02 mM; $q_{Cr^{3+}}$ = 1.2 mmol g^{-1}); 4 – Cr(III)-loaded biomass (fresh protonated biomass was equilibrated with a Cr(III) solution ([Cr(III)]$_0$ = 1.2 mmol L^{-1}) at pH = 4.0 obtained by reduction of a Cr(VI) solution, $q_{Cr^{3+}}$ = 0.4 mmol g^{-1}).
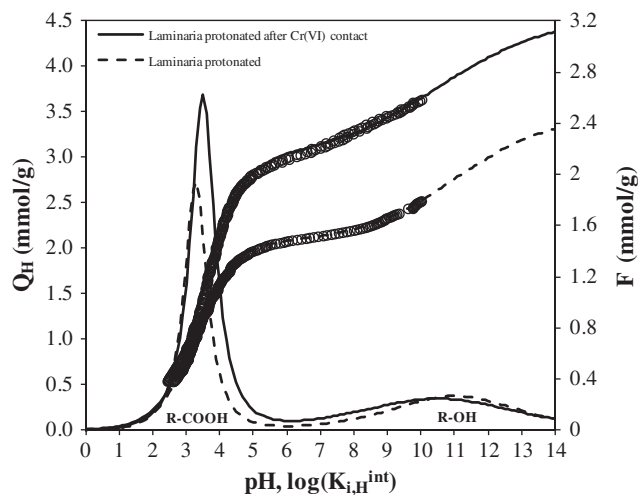

Fig. 2. Experimental data and model curves for biosorbent potentiometric titrations and affinity distribution function for hydrogen ions, $F = \sum_i f_i(\log K_{i,H}^{int}) Q_{max,i}$. (—) before and (- -) after Cr(VI) oxidation.

Table 1
Continuous distribution model parameters for the brown alga *Laminaria digitata* (IS = 0.1 M).

Algal sample	$Q_{max,1}$ (mmol g^{-1})	$Q_{max,2}$ (mmol g^{-1})	$pK'_{1,H}$	$pK'_{2,H}$	$m_{H,1}$	$m_{H,2}$	R^2	S_R^2 (mmol g^{-1})^2
Protonated	2.06 ± 0.01	1.4 ± 0.7	3.28 ± 0.01	11 ± 1	0.77 ± 0.01	0.31 ± 0.05	0.999	2.7×10^{-4}
Cr loaded[a]	2.97 ± 0.09	1.6 ± 0.9	3.49 ± 0.01	10 ± 3	0.75 ± 0.02	0.3 ± 0.1	0.997	2.4×10^{-3}

[a] Algae sample after Cr(VI) reduction ([Cr(VI)]$_0$ = 6.2 mM; 4 g biomass L^{-1}, contact time = 143 h; [Cr(VI)]$_{final}$ = 0.02 mM; X_{OXI} = 0.74; [Cr(III)]$_{final}$ = 0.98 mM; $q_{Cr^{3+}}$ = 1.2 mmol g^{-1}).

4.3. Kinetic modeling of Cr(VI) reduction to Cr(III)

4.3.1. Influence of pH

Fig. 3a shows that the kinetic model, presented in Section 2.2, is able to fit well the Cr(VI) reduction for all the pH values tested. Fig. 3a also confirms the important role played by solution pH in Cr(VI) reduction, in which strongly acidic conditions favor the reduction rates (Table 2). Although Cr(VI) reduction is observed in the all range of pH tested, the reaction rate at pH = 1.0 is more than 100 times higher than at pH 4.0, since protons are needed for the reduction of hexavalent chromium to trivalent chromium, according to Eqs. (4)–(8). At pH 1.0, only 8 h are required for complete Cr(VI) removal considering the detection limit of the analytical method (<10 μg L^{-1}).

Park et al. [33] also demonstrated that the reaction rate constant is strongly pH dependent, and that a linear correlation exists between the reaction rate logarithm and the pH value, according to Eq. (20):

$$k = f([H^+]) = a[H^+]^n, \quad \log k = \log a - n \times pH \tag{20}$$

where n is the order of the reaction with respect to proton concentration and a is an empirical constant. Eq. (20) fits well to experimental data (Fig. B – Supplementary data file), yielding n and a values of 0.72 ± 0.08 and 400 ± 200 L^{n+1} mol$^{-(n+1)}$ h^{-1}, respectively. This indicates that the hexavalent chromium reduction reaction is approximately a first order reaction with respect to protons concentration ($n \sim 1$). Park et al. [33] obtained the same value, n = 0.714, for the Cr(VI) reduction using the brown seaweed *Ecklonia sp.*

Fig. 3b shows that Cr(VI) concentration decreases with time and is completely removed, below the detection limit, from the aqueous phase, after 52 h at pH = 2.5. In other hand, Cr(III), which was not initially present neither in the aqueous solution or in solid phase (biomaterial), appears in the aqueous phase and its concentration increases until all Cr(VI) is removed. However, this increase is not proportional to the Cr(VI) disappearance, as part of the Cr(III) sorbs onto the surface of the biosorbent. This indicates that Cr(VI) was directly reduced to Cr(III) in the aqueous phase by contact with electron–donor groups of the biomass, and the reduced Cr(III) established an equilibrium between the liquid and solid phase, in which Cr(III) binds to the negatively charged groups present in the surface of the biomaterial. Park et al. [15] showed that chromium bound on fifteen biomaterials (*Sargassum*, *Ecklonia*, pine bark, pine cone, banana skin, pine needle, walnut shell, rice straw, *Rhizopus*, etc.) was mostly or totally in trivalent form, for an initial pH of 2.2, using high-resolution XPS technique.

A significant amount of dissolved organic matter was released into the system, confirmed by the DOC analysis in the aqueous solution, mainly due to the biomass oxidation during Cr(VI) reduction. At the end of the Cr(VI) reduction reactions DOC values of 232.6 mg L^{-1} (reaction time = 143 h, [Cr(VI)]$_0$ = 321 mg L^{-1}, [Cr(VI)]$_{final}$ = 1.2 mg L^{-1}, X_{OXI} = 0.74, T = 25 °C, [B] = 4 g L^{-1}) and 345 mg L^{-1} (reaction time = 47 h, [Cr(VI)]$_0$ = 278 mg L^{-1}, [Cr(VI)]$_{final}$ = 0.029 mg L^{-1}, X_{OXI} = 0.63, T = 25 °C, [B] = 4 g L^{-1}) were achieved for the experiments performed at pH 2.5 and 1.0, respectively. Turbidity in the solution was observed after longer contact times, >120 h, and principally for pH > 3.0, associated to the release of organic compounds from the biomass by oxidation and dissolution of some algae extracts [43]. Table 3 summarizes the values for the volatile matter, TOC and Cr present in the solid matter after Cr(VI) reduction at pH 2.5 and 1.0 with an initial Cr(VI) concentration of 6.2 mM and 5.3 mM, respectively (T = 20 °C, [B] = 4 g L^{-1}) and compares with the values for the protonated algae. This shows that even for the most severe conditions (pH 1.0) the oxidation process does not achieve significant mineralization of biomass organic matter. The algae sample, oxidized at pH 2.5, showed a high percentage of ash (9.8%) when compared with the protonated algae (0.5%) [37], which can be attributed to the high level of chromium adsorbed during the reduction process. After the reduction at pH 1.0, the algae had low ash content (1.9%) due to the small amount of chromium adsorbed at this pH value. The results presented for Cr adsorbed at pH 2.5 and 1.0 are slightly lower than those obtained from the material balance in the reactor during the kinetic studies (66.4 mg g^{-1} and 5.5 mg g^{-1}, respectively), suggesting a partial loss of chromium during the biomass digestion procedure.

In the biomass limited experiment ([Cr(VI)]$_0$ = 4.2 mmol L^{-1}, [Cr(VI)]$_{final}$ = 1.9 mmol L^{-1}, [B] = 1.1 g L^{-1}, T = 20 °C, contact time = 42 days), 1 g of the biomass was able to reduce 2.1 mmol of Cr(VI) (109.2 mg) at pH 2.5. Considering that at pH 2.5, and in the range of hexavalent chromium concentrations used, the molar fractions of HCrO$_4^-$, CrO$_7^{2-}$ and H$_2$CrO$_4$ are 84.5%, 15.2% and 0.2%, respectively, and since 3, 6 and 3 mmol of electrons are required for the reduction of 1 mmol of Cr(VI) to Cr(III), respectively for HCrO$_4^-$, CrO$_7^{2-}$ and H$_2$CrO$_4$ species, it can be suggested that 1 g of biomass has 7.25 mmol of available electrons. Considering that, in theory, 1 g of FeSO$_4$·7H$_2$O can reduce 62.4 mg of Cr(VI) (1.2 mmol), the Cr(VI)-reducing capacity of algae *L. digitata* is almost two times higher than that of the common chemical Cr(VI)-reductant. Table 4 compares the reducing capacities for different biomaterials tested, and it can be seen that algae *L. digitata* shows to be an interesting biomaterial for these kinds of applications.

Although the Cr(VI) reduction rates increases sharply with the decrease of solution pH, the removal of total chromium has an optimum pH value for a fixed contact time, as it can be observed in Fig. 3c. The removal efficiency of total chromium was calculated from the mass balance for total Cr in the aqueous phase. Fig. 3c shows that the optimum pH for total Cr removal increases with the contact time until pH 3.0. This observation can be attributed to three main factors: (i) at a high pH, Cr(VI) reduction rate is very slow, and can be considered the rate limiting step mainly due to the protons limitation, and as the contact time increases, Cr(VI) can be completely reduced to Cr(III), which is then bound to the negatively charged functional groups present on the surface of the biomaterial; (ii) increasing the solution pH, sorption of Cr(III) is favored since more deprotonated negatively charged groups are available and the competition between protons and trivalent chromium ions for actives sites decreases, (iii) at pH above 3.0 the protons in solution are not sufficient for the reduction reaction to occur, during the reaction period tested, and low amount of trivalent chromium are generated, decreasing the total Cr removal efficiency. Park et al. [6] also observed the same phenomenon for Cr(VI) removal using the brown seaweed *Ecklonia*, obtaining an
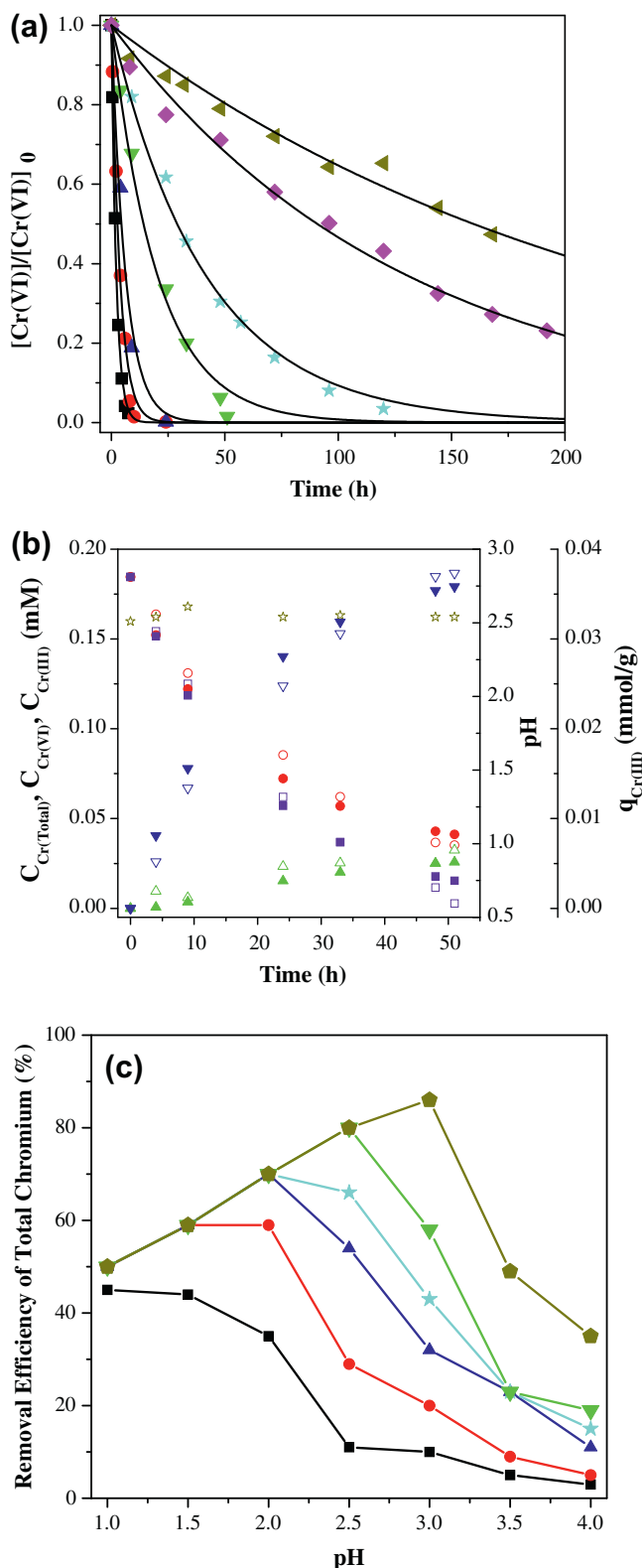
Fig. 3. (a) Evolution of Cr(VI) concentration as a function of time at various pH values: (■) – pH = 1.0, (●) – pH = 1.5, (▲) – pH = 2.0, (▼) – pH = 2.5, (★) – pH = 3.0, (◆) – pH = 3.5, (◄) – pH = 4.0; Symbols: experimental data; Line: predicted data. (b) Evolution of Cr(VI), Cr(III) and total Cr concentrations and trivalent chromium uptake over time at controlled pH (2.5): (☆): pH; (□, ■): $C_{Cr(VI)}$; (△, ▲): $C_{Cr(III)}$; (○, ●): $C_{Cr(total)}$; (▽, ▼): $q_{Cr(III)}$; Conditions: $[Cr(VI)]_0 = 0.2$ mmol L^{-1}, $[B] = 4$ g L^{-1}, $T = 20$ °C; Open symbols: experimental data; Closed symbols: predicted data. (c) Optimum pH for the removal efficiency of total Cr according to the reaction time; Symbols: (■) – 4 h, (●) – 9 h, (▲) – 24 h, (★) – 32 h, (▼) – 48 h, (⬟) – 120 h; Conditions: $[Cr(VI)]_0 = 0.2$ mmol L^{-1}, $[B] = 4$ g L^{-1}, $T = 20$ °C.

optimum pH value according to the reaction time. For reaction times of 48 h and 480 h, the optimum pH value was 3.0 and 4.0, respectively.

4.3.2. Effect of initial Cr(VI) concentration

Fig. 4a shows that higher initial Cr(VI) concentrations requires longer contact times, ranging from 40 to 140 h, respectively for the lowest and highest initial Cr(VI) concentrations tested, to achieve final Cr(VI) concentrations below the analytical detection limit (<10 μg L^{-1}). However, the initial Cr(VI) concentration, considering the concentration range between 0.2 and 6.2 mM, had little influence on the Cr(VI) removal rate (Table 2), and the obtained results shows that Cr(VI) reduction is a first-order reaction with respect to the Cr(VI) concentration. On the other hand, considering that the biomaterial has a limited number of organic compounds with capacity to reduce Cr(VI), which means a limited number of electrons for Cr(VI) doses higher than 2.1 mmol per gram of biomaterial, insufficient electrons will be available for total Cr(VI) conversion into Cr(III).

Higher initial Cr(VI) concentrations results in higher Cr(III) concentrations released to the solution, leading to higher amounts of Cr(III) accumulated in the biomaterial. Considering that the sorption rate of the reduced Cr(III) might be faster than the reduction rate of Cr(VI) for pH values above 2.0, as observed in a previous work using pure solutions of Cr(III) [36], where the equilibrium is achieved after 10 h, it can be assumed that the reduced Cr(III) remains in equilibrium between the liquid and solid phase. Fig. 5 shows the Cr(III) equilibrium data points obtained during Cr(VI) reduction (the biomass is oxidized during the Cr(VI) reduction to Cr(III)) (experimental and model prediction using Eq. (18)) and using pure Cr(III) solutions (in contact with fresh protonated biomass). Considering the equilibrium data obtained at pH 2.5, the uptake capacity of Cr(III) is four times higher for the reduced Cr(III) solution (the oxidation of the biomass during Cr(VI) reduction was 73%), than for pure Cr(III) solutions. These results are in agreement with the potentiometric titration data, where it was concluded an increment of carboxylic groups during the oxidation of the biomass.

Fig. 4b shows that the kinetic model, considering integrated reduction reactions and sorption processes is able to fit well the concentration profiles of Cr(VI), Cr(III), total Cr and trivalent chromium uptake over time. The pH was not modeled, since pH was controlled during the reaction.

4.3.3. Effect of biomass concentration

Fig. 6 shows the Cr(VI) reduction kinetics using different biomass concentration in the range of 0.5–6.0 g L^{-1}, for an initial Cr(VI) concentration of 0.2 mM, pH controlled at 2.5 and a temperature of 20 °C. The kinetic model fits well the Cr(VI) reduction kinetics for all tested biomass concentrations. Although Cr(VI) removal rates increases with increasing biosorbent dose, since more electrons are available for the reduction reaction, for biomass concentrations higher than 4 g L^{-1}, the reaction rate decreases slightly mainly associated to high density of solids that difficult the interaction of Cr(VI) anions with the biomass surface. For lower biomass doses, the limiting reaction step is the availability of electrons. Although total chromium removal is similar (~81%) for all biomass concentrations tested, lower reaction times are necessary when using higher biomass doses.

4.3.4. Temperature effect

Fig. 7 shows the temperature dependency of Cr(VI) reduction reaction, in the range of 10–40 °C, at a fixed pH value and biomass concentration of 2.5 and 4 g L^{-1}, respectively. The Cr(VI) reduction reaction was greatly dependent on the solution temperature, leading to a substantial reduction of contact time, necessary to

Table 2
Estimated kinetic model parameters for Cr(VI) reduction (values ± standard deviation).

pH	$[B]$ (g L^{-1})	T (°C)	$[Cr(VI)]_0$ (mM)	Total chromium removal (%)	Contact time (h)	k (L mmol^{-1} h^{-1}) × 10^2	R^2	S_R^2 (mmol L^{-1})^2
1.0	4	20	0.21	51	8	5.6 ± 0.4	0.998	1.1 × 10^{-5}
1.5				59	24	3.2 ± 0.5	0.990	6.8 × 10^{-5}
2.0				74	24	1.9 ± 0.4	0.988	1.0 × 10^{-4}
2.5				81	51	0.59 ± 0.08	0.991	4.5 × 10^{-5}
3.0				86	120	0.29 ± 0.02	0.995	2.1 × 10^{-5}
3.5				71	216	0.091 ± 0.006	0.990	2.8 × 10^{-5}
4.0				50	168	0.052 ± 0.004	0.969	3.3 × 10^{-5}
2.5	4	20	0.21	81	51	0.59 ± 0.08	0.991	4.54 × 10^{-5}
			0.97	88	57	0.81 ± 0.08	0.995	6.33 × 10^{-4}
			6.19	84	143	0.90 ± 0.04	0.999	7.92 × 10^{-3}
2.5	0.5	20	0.21	78	168	1.4 ± 0.2	0.976	1.2 × 10^{-4}
	1.0			79	120	0.9 ± 0.2	0.964	2.2 × 10^{-4}
	2.0			83	72	0.83 ± 0.08	0.999	3.2 × 10^{-6}
	4.0			81	51	0.59 ± 0.08	0.991	4.5 × 10^{-5}
	6.0			86	48	0.69 ± 0.03	0.990	4.2 × 10^{-5}
2.5	4.0	10	0.21	81	76	0.45 ± 0.05	0.992	4.51 × 10^{-5}
		20	0.21	81	51	0.59 ± 0.08	0.991	4.54 × 10^{-5}
		30	0.18	83	24	1.4 ± 0.1	0.993	2.53 × 10^{-5}
		40	0.19	80	12	2.6 ± 0.2	0.994	2.69 × 10^{-5}

Table 3
Volatile content, TOC and Cr present in the seaweed before and after Cr(VI) reduction at pH 2.5 ($[Cr(VI)]_0$ = 6.2 mM; $[Cr(VI)]_{final}$ = 0.02 mM; $[B]$ = 4 g L^{-1}; T = 20 °C; Contact time = 143 h) and pH 1.0 ($[Cr(VI)]_0$ = 5.3 mM; $[Cr(VI)]_{final}$ = 0.003 mM; $[B]$ = 4 g L^{-1}; T = 20 °C; Contact time = 47 h).

Sample	Volatile (%)	Ash (%)	TC = TOC[a] (mg C g^{-1})	[Cr] (mg g^{-1})
Protonated [37]	99.5 ± 0.1	0.5 ± 0.1	410 ± 10	(4.0 ± 0.3) × 10^{-3}
Oxidized at pH 2.5	90.2 ± 0.1	9.8 ± 0.1	350 ± 1	62 ± 3
Oxidized at pH 1.0	98.1 ± 0.1	1.8 ± 0.1	398 ± 1	4.1 ± 0.2

[a] Inorganic carbon was negligible; TC – total carbon; TOC – total organic carbon.

Table 4
Cr(VI) reducing capacity for different biomaterials.

Biomaterial	C_{OC}^* (mmol g^{-1})	References
Laminaria digitata	2.10	This study
Sargassum	1.62	[7]
Ecklonia	4.49	[6]
Banana skin	4.89	[29]
Fermentation waste	0.24	[47]
Mangrove Leaves	0.17	[32]
Pine cone	1.11	[15]
Sugarcane Bagasse	0.25	[48]

achieve complete removal of Cr(VI) below the detection limit of the analytical method, as the solution temperature increases. This can be mainly attributed to two main factors: (i) the increase of the solution reduction potential with temperature [44]; (ii) the increase of diffusion rate of ions from the bulk solution to the surface of biosorbent with temperature [45].

The kinetic model was able to fit well the experimental data at different temperatures, showing an increase of the kinetic rate constant of about five times from 20 °C to 40 °C (Table 2). The percentage of total Cr removal was similar for all kinetics performed at different temperatures (~80%), which means that the increase in temperature does not enhance the adsorption capacity (in all experiments almost complete reduction of Cr(VI) to Cr(III) was achieved, meaning that the same concentration of trivalent chromium was equilibrated with the biomass).

The influence of the temperature on the reaction rate can be expressed mathematically by the Arrhenius equation [46]:

$$k = Ae^{-\frac{Ea}{RT}} \text{ or } \ln k = \ln A - \frac{E_a}{R}\frac{1}{T} \tag{21}$$

where A, E_a, R, T and k are the frequency factor, activation energy (J mol^{-1}), gas constant (8.314 J mol^{-1} K^{-1}), temperature in Kelvin

(K) and kinetic constant (L mol^{-1} h^{-1}), respectively. The activation energy obtained for the removal of Cr(VI) by *L. digitata* was 45 ± 20 kJ mol^{-1} (Fig. C – Supplementary data file). The value for $\ln A$ (L mol^{-1} h^{-1}) was 20 ± 8. The values obtained were in the same order of magnitude as those reported by Park et al. [34] in the Cr(VI) removal using the biomaterial pine needle.

4.4. Total chromium concentration modeling

Total and trivalent concentration profiles can be only predicted if trivalent chromium equilibrium is known. Considering that carboxylic groups are the main responsible for Cr(III) binding, and that during the hexavalent chromium reduction, and consequently oxidation of the biomass, the number of negatively groups available for the trivalent chromium binding increases, the equilibrium model proposed is described by Eq. (18). Although the equilibrium equation fits well the experimental data obtained at different Cr(III) equilibrium concentrations (pH = 2.5) (Fig. 5) and at different biomass concentrations (data not presented), the model overestimated the Cr(III) uptake capacity at pH values higher than 2.5. This can be attributed to the fact, that in those situations, the equilibrium time (Cr(VI) reaction time) was not sufficient to reach the Cr(III) equilibrium between the solid and liquid phase. The estimated model equilibrium parameters for trivalent chromium biosorption are shown in Table 5. The pK_H and pK_{Cr} values are lower than those obtained for the Cr(III) biosorption using pure Cr(III) solutions [36], which indicates that protons and Cr(III) ions may be complexed with the organic matter released during Cr(VI) reduction and the overall affinity of the organic-metal complex to the binding groups decreases. The same conclusions were obtained from the experiment, in which an amount of protonated biomass was in contact with a Cr(III) solution obtained from Cr(VI) solution, and the uptake capacity of Cr(III) was lower than that observed
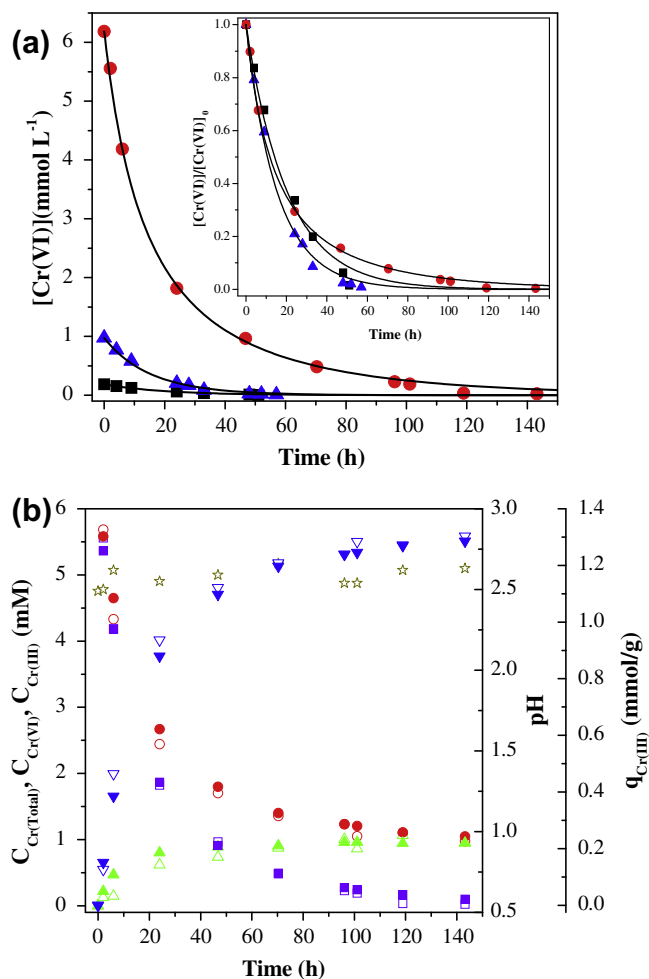
Fig. 4. (a) Evolution of Cr(VI) concentration as a function of time at various $[Cr(VI)]_0$: ($\blacksquare$) – $[Cr(VI)]_0 = 0.21$ mmol L^{-1}, ($\blacktriangle$) – $[Cr(VI)]_0 = 0.98$ mmol L^{-1}, ($\bullet$) – $[Cr(VI)]_0 = 6.19$ mmol L^{-1}; Conditions: $[Cr(VI)]_0 = 0.2$ mmol L^{-1}, $[B] = 4$ g L^{-1}, $T = 20$ °C; Symbols: experimental data; Line: predicted data. (b) Evolution of Cr(VI), Cr(III) and total Cr concentrations and trivalent chromium uptake capacity over time at controlled pH (2.5): ($\star$): pH; ($\square$, $\blacksquare$): $C_{Cr(VI)}$; ($\triangle$, $\blacktriangle$): $C_{Cr(III)}$; ($\circ$, $\bullet$): $C_{Cr(total)}$; ($\triangledown$, $\blacktriangledown$): $q_{Cr(III)}$; Conditions: $[Cr(VI)]_0 = 6.19$ mmol L^{-1}; $[B] = 4$ g L^{-1}, $T = 20$ °C; Open symbols: experimental data; Closed symbols: predicted data.

during the Cr(VI) reduction. This also indicates, that during the Cr(VI) reduction, a faction of Cr(III) ions bounds to the functional groups immediately without interaction of the organic matter released to the solution. Another important aspect is that the *f* value is higher than one, meaning that new negatively charged binding sites are generated during Cr(VI) reduction, and it depends on the degree of biomass oxidation. A higher biomass oxidation leads to higher amount of negatively charged binding groups.

Figs. 3b and 4b shows that the mass balance to the total chromium is well predicted, as well the trivalent chromium concentration in the solid and liquid phase.

The Cr(III) interference on Cr(VI) reduction was also evaluated (Fig. D – Supplementary data file). The reaction rate for Cr (VI) removal is not influenced by Cr(III) concentration in the solution. Park et al. [6] demonstrated the irreversibility of the reaction of Cr(VI), considering the effect of Cr(III) concentration (0, 50 and 100 mg L^{-1}) in the Cr(VI) reduction at pH 1.0.

5. Conclusion

The protonated brown seaweed *L. digitata* showed to be an effective biomass for the reduction of hexavalent chromium from
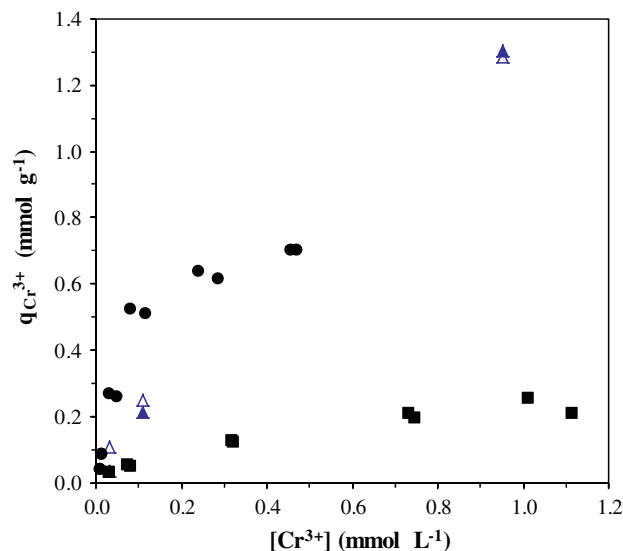

Fig. 5. Equilibrium isotherms of trivalent chromium sorption: reduced Cr(III) solution during Cr(VI) reduction at pH ~ 2.6 ($\blacktriangle$ – experimental data; $\triangle$ – equilibrium model); pure Cr(III) solutions at pH 4.0 ($\bullet$) and 2.5 ($\blacksquare$) using fresh protonated biomass [36].
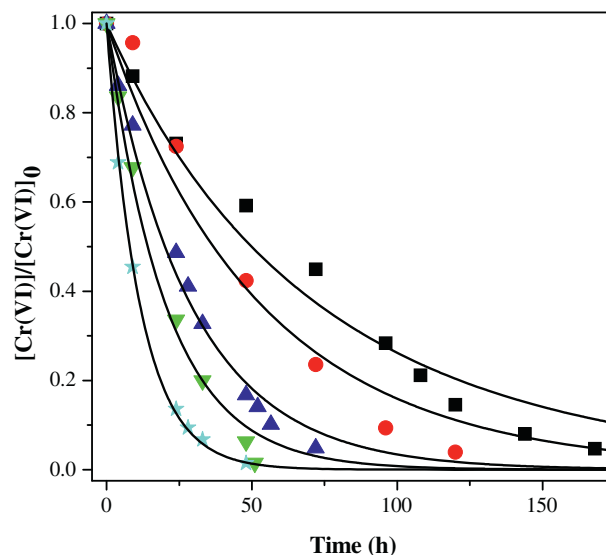
Fig. 6. Evolution of Cr(VI) concentration as a function of time at different biomass concentrations: ($\blacksquare$) – 0.5 g L^{-1}, ($\bullet$) – 1.0 g L^{-1}, ($\blacktriangle$) – 2.0 g L^{-1}, ($\star$) – 4.0 g L^{-1}, ($\blacktriangleleft$) – 6.0 g L^{-1}; Conditions: $[Cr(VI)]_0 = 0.2$ mmol L^{-1}, pH = 2.5, $T = 20$ °C; Symbols: experimental data; Line: predicted data.

aqueous solutions and trivalent chromium sorption. The FTIR spectra showed that the biomass oxidation during the Cr(VI) reduction and Cr(III) accumulation in the biomass, changes the absorption frequencies of the various functional groups present in the surface of the biomass. The potentiometric titration revealed a substantial increase on the number of carboxylic groups during the biomass oxidation, which was later correlated with the increase on the Cr(III) uptake capacity. Cr(VI) elimination by protonated *Laminaria* was mainly associated to the direct reduction mechanism, in which Cr(VI) was directly reduced to Cr(III) in the aqueous phase by contact with electron-donor groups of the biomass, and the reduced Cr(III) remained in the aqueous phase or bounded to the negatively charged carboxylic groups. The concentration of equivalent organic compounds, per unit gram of biomaterial, with capacity to reduce
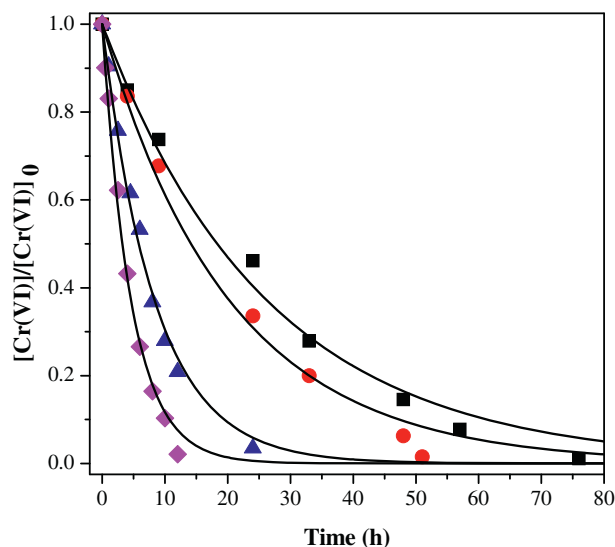
Fig. 7. Evolution of Cr(VI) concentration as a function of time at different temperatures: (■) – $T = 10\,°C$, (●) – $T = 20\,°C$, (▲) – $T = 30\,°C$, (◆) – $T = 40\,°C$; Conditions: $[Cr(VI)]_0 = 0.2\ mmol\ L^{-1}$, $[B] = 4\ g\ L^{-1}$, pH = 2.5; Symbols: experimental data; Line: predicted data.

Table 5
Estimated model equilibrium parameters for trivalent chromium biosorption onto brown alga *Laminaria digitata*.

$pK'_{Cr^{3+}}$	pK'_H	f	R^2	S_R^2 $(mmol\ g^{-1})^2$
3 ± 1	2 ± 1	6 ± 4	0.987	3.8×10^{-4}

$[B]_T = Q_{max,1} = 2.06\ mmol\ g^{-1}$; $C_{OC}^* = 2.1\ mmol\ g^{-1}$; $K'_H = 1/K_H$; $K'_{Cr^{3+}} = 1/K_{Cr^{3+}}$.

Cr(VI), is $2.1\ mmol\ g^{-1}$. Considering the molar fractions of Cr(VI) species and the required number of electrons for each species, 1 g of biomass has 7.25 mmol of available electrons, indicating that the Cr(VI)-reducing capacity of algae *L. digitata* is almost two times higher than that of the common chemical Cr(VI)-reductant (ferrous sulfate). The rate of Cr(VI) reduction was highly pH dependent since protons are involved in the redox reaction. Although low pH values enhance significantly the Cr(VI) reduction rate, Cr(III) sorption is drastically reduced since the functional groups become protonated, leading to low total chromium removal efficiency. The optimum pH value for total chromium removal was 2.5 and 3.0 for reaction times of 48 h and 140 h, respectively, indicating that the reduction reaction is the limiting step of the overall process. The solution temperature enhances significantly the Cr(VI) reduction rate, achieving a five holder increase from 10 °C to 40 °C, leading to an activation energy of $45 ± 20\ kJ\ mol^{-1}$.

The kinetic model fitted well all the experimental data at different conditions of pH, temperature, biomass concentration and Cr(VI) concentration. This indicates that the hexavalent chromium reduction reaction is approximately first order with respect to Cr(VI) and concentration of OC with capacity to reduce Cr(VI) to Cr(III).

Acknowledgments

Appendix A. Supplementary material

Supplementary data associated with this article can be found, in the online version, at http://dx.doi.org/10.1016/j.cej.2013.10.051.

References

[1] B. Saha, C. Orvig, Biosorbents for hexavalent chromium elimination from industrial and municipal effluents, Coordination Chemistry Reviews 254 (2010) 2959–2972.
[2] A.K. Shanker, C. Cervantes, H. Loza-Tavera, S. Avudainayagam, Chromium toxicity in plants, Environment International 31 (2005) 739–753.
[3] J.F. Cárdenas-González, I. Acosta-Rodríguez, Hexavalent Chromium Removal by a *Paecilomyces sp.* Fungal strain isolated from environment, Bioinorganic Chemistry and Applications 2010 (2010) 133–150.
[4] J. Kotas, Z. Stasicka, Chromium occurrence in the environment and methods of its speciation, Environmental Pollution 107 (2000) 263–283.
[5] E.W. Odenkrichen, R. Eisler, Chlorpyrifos hazards to fish, wildlife, and invertebrates: a synoptic review, in: US Fish and Wildlife Service Biological Report 85, (1.13), Contaminant Hazard Reviews, Report No. 13, 1988, pp. 1–38.
[6] D. Park, Y.-S. Yun, J.M. Park, Reduction of hexavalent chromium with the brown seaweed *Ecklonia* biomass, Environmental Science & Technology 38 (2004) 4860–4864.
[7] D. Kratochvil, P. Pimentel, B. Volesky, Removal of trivalent and hexavalent chromium by seaweed biosorbent, Environmental Science & Technology 32 (1998) 2693–2698.
[8] Z. Ai, Y. Cheng, L. Zhang, J. Qiu, Efficient removal of Cr(VI) from aqueous solution with Fe@Fe$_2$O$_3$ core–shell nanowires, Environmental Science & Technology 42 (2008) 6955–6960.
[9] S. Bosinco, J. Roussy, E. Guibal, P. Lecloirec, Interaction mechanisms between heavalent chromium and corncob, Environmental Technology 17 (1996) 55–62.
[10] D.C. Sharma, C.F. Forster, Removal of hexavalent chromium using sphagnum moss peat, Water Research 27 (1993) 1201–1208.
[11] X.S. Wang, Y.P. Tang, S.R. Tao, Kinetics, equilibrium and thermodynamic study on removal of Cr(VI) from aqueous solutions using low-cost adsorbent Alligator weed, Chemical Engineering Journal 148 (2009) 217–225.
[12] G. Moussavi, B. Barikbin, Biosorption of chromium(VI) from industrial wastewater onto pistachio hull waste biomass, Chemical Engineering Journal 162 (2010) 893–900.
[13] J.L. Gardea-Torresdey, K.J. Tiemann, V. Armendariz, L. Bess-Oberto, R.R. Chianelli, J. Rios, J.G. Parsons, G. Gamez, Characterization of Cr(VI) binding and reduction to Cr(III) by the agricultural byproducts of Avena monida (Oat) biomass, Journal of Hazardous Materials 80 (2000) 175–188.
[14] M.F. Sawalha, J.L. Gardea-Torresdey, J.G. Parsons, G. Saupe, J.R. Peralta-Videa, Determination of adsorption and speciation of chromium species by saltbush (*Atriplex canescens*) biomass using a combination of XAS and ICP–OES, Microchemical Journal 81 (2005) 122–132.
[15] D. Park, S.-R. Lim, Y.-S. Yun, J.M. Park, Reliable evidences that the removal mechanism of hexavalent chromium by natural biomaterials is adsorption-coupled reduction, Chemosphere 70 (2007) 298–305.
[16] V.W. Truesdale, The biogeochemical effect of seaweeds upon close-to natural concentrations of dissolved iodate and iodide in seawater – preliminary study with *Laminaria digitata* and *Fucus serratus*, Estuarine, Coastal and Shelf Science 78 (2008) 155–165.
[17] N.C. Moroney, M.N. O'grady, J.V. O'doherty, J.P. Kerry, Effect of a brown seaweed (*Laminaria digitata*) extract containing laminarin and fucoidan on the quality and shelf-life of fresh and cooked minced pork patties, Meat Science 94 (2013) 304–311.
[18] P. Vauchel, K. Leroux, R. Kaas, A. Arhaliass, R. Baron, J. Legrand, Kinetics modeling of alginate alkaline extraction from *Laminaria digitata*, Bioresource Technology 100 (2009) 1291–1296.
[19] R. Sips, On the structure of a catalyst surface, Journal of Chemical Physics 16 (1948) 490–495.
[20] L.K. Koopal, T. Saito, J.P. Pinheiro, W.H.V. Riemsdijk, Ion binding to natural organic matter: general considerations and the NICA-Donnan model, Colloids and Surfaces A: Physicochemical and Engineering Aspects 265 (2005) 40–54.
[21] C.J. Milne, D.G. Kinniburgh, J.C.M. De Wit, W.H. Van Riemsdijk, L.K. Koopal, Analysis of proton binding by a peat humic acid using a simple electrostatic model, Geochimica et Cosmochimica Acta 59 (1995) 1101–1112.
[22] S.C. Chapra, R.P. Canale, Numerical Methods for Engineers, third ed., McGraw-Hill, Singapore, 1998. pp. 463–471.
[23] G. Cainelli, G. Cardillo, Chromium Oxidations in Organic Chemistry, in: K. Hafner, J.-M. Lehn, C.W. Rees, P.V. Rague Schleyer, B.M. Trost, R. Zahradnik (Eds.), Reactivity and Structure: Concepts in Organic Chemistry, vol. 19, Springer Heidelberg, Berlin, 1984, pp. 1–7.
[24] L.K. Cabatingan, R.C. Agapay, J.L.L. Rakels, M. Ottens, L.a.M.V.D. Wielen, Potential of biosorption for the recovery of chromate in industrial

wastewaters, Industrial & Engineering Chemistry Research 40 (2001) 2302–2309.

[25] D. Park, Y.-S. Yun, J. Hye Jo, J.M. Park, Mechanism of hexavalent chromium removal by dead fungal biomass of *Aspergillus niger*, Water Research 39 (2005) 533–540.

[26] D. Park, Y.-S. Yun, J.M. Park, Studies on hexavalent chromium biosorption by chemically-treated biomass of *Ecklonia sp.*, Chemosphere 60 (2005) 1356–1364.

[27] D. Park, Y.-S. Yun, J.M. Park, Use of dead fungal biomass for the detoxification of hexavalent chromium: screening and kinetics, Process Biochemistry 40 (2005) 2559–2565.

[28] D. Park, Y.-S. Yun, J.M. Park, Mechanisms of the removal of hexavalent chromium by biomaterials or biomaterial-based activated carbons, Journal of Hazardous Materials 137 (2006) 1254–1257.

[29] D. Park, S.-R. Lim, Y.-S. Yun, J.M. Park, Development of a new Cr(VI)-biosorbent from agricultural biowaste, Bioresource Technology 99 (2008) 8810–8818.

[30] E. Nishide, H. Anzai, N. Uchida, Extraction of alginic acid from a Brazilian brown alga, Laminaria brasiliensis, in: M. Ragan, C. Bird (Eds.), Twelfth International Seaweed Symposium, Hydrobiologia 151/152.551-555, Springer, Netherlands, 1987, pp. 551–555.

[31] L. Dupont, E. Guillon, Removal of hexavalent chromium with a lignocellulosic substrate extracted from wheat bran, Environmental Science & Technology 37 (2003) 4235–4241.

[32] R. Elangovan, L. Philip, K. Chandraraj, Biosorption of chromium species by aquatic weeds: kinetics and mechanism studies, Journal of Hazardous Materials 152 (2008) 100–112.

[33] D. Park, Y.-S. Yun, C.K. Ahn, J.M. Park, Kinetics of the reduction of hexavalent chromium with the brown seaweed Ecklonia biomass, Chemosphere 66 (2007) 939–946.

[34] D. Park, Y.-S. Yun, H.W. Lee, J.M. Park, Advanced kinetic model of the Cr(VI) removal by biomaterials at various pHs and temperatures, Bioresource Technology 99 (2008) 1141–1147.

[35] V.J.P. Vilar, J.A.B. Valle, A. Bhatnagar, J.C. Santos, S.M.A. Guelli, U. De Souza, A.A.U. De Souza, C.M.S. Botelho, R.A.R. Boaventura, Insights into trivalent chromium biosorption onto protonated brown algae *Pelvetia canaliculata*: distribution of chromium ionic species on the binding sites, Chemical Engineering Journal 200–202 (2012) 140–148.

[36] I.M. Dittert, V.J.P. Vilar, E.A.B. Silva, S.M.A.G. Souza, A.A.U. De Souza, C.M.S. Botelho, R.A.R. Boaventura, Turning *Laminaria digitata* seaweed into a resource for sustainable and ecological removal of trivalent chromium ions from aqueous solutions, Clean Technology and Environmental Policy (2012) 1–11.

[37] I.M. Dittert, V.J.P. Vilar, E.A.B. Da Silva, S.M.A.G. De Souza, A.A.U. De Souza, C.M.S. Botelho, R.A.R. Boaventura, Adding value to marine macro-algae *Laminaria digitata* through its use in the separation and recovery of trivalent chromium ions from aqueous solution, Chemical Engineering Journal 193–194 (2012) 348–357.

[38] Y.-S. Yun, D. Park, J.M. Park, B. Volesky, Biosorption of trivalent chromium on the brown seaweed biomass, Environmental Science & Technology 35 (2001) 4353–4358.

[39] L.S. Clesceri, A.E. Greenberg, A.D. Eaton, Standard Methods for Examination of Water & Wastewater, 20th ed., American Public Health Association (APHA), American Water Works Association (AWWA) & Water Environment Federation (WEF), Washington, DC, 1998.

[40] P.X. Sheng, Y.-P. Ting, J.P. Chen, L. Hong, Sorption of lead, copper, cadmium, zinc, and nickel by marine algal biomass: characterization of biosorptive capacity and investigation of mechanisms, Journal of Colloid and Interface Science 275 (2004) 131–141.

[41] E. Fourest, B. Volesky, Contribution of sulfonate groups and alginate to heavy metal biosorption by the dry biomass of sargassum fluitans, Environmental Science & Technology 30 (1995) 277–282.

[42] E.H. Reith, E.P. Deurwaarder, K. Hemmes, A.P.W.M. Curvers, P. Kamermans, W.A. Brandenburg, G. Lettings, BIO-OFFSHORE: Grootschalige teelt van zeewieren in combinatie met offshore windparken in de Noordzee, in, Wageningen, Energy Research in the Netherlands (ECN), Petten & Wageningen University and Research Centre, Petten, 2005. p. 110.

[43] T.A. Davis, B. Volesky, A. Mucci, A review of the biochemistry of heavy metal biosorption by brown algae, Water Research 37 (2003) 4311–4330.

[44] W. Stumm, J.J. Morgan, Aquatic Chemistry: Chemical Equilibria and Rates in Natural Waters, third ed., John Wiley & Sons, Inc., New York, 1996. pp. 443–444.

[45] T.S. Kassem, Kinetics and thermodynamic treatments of the reduction of hexavalent to trivalent chromium in presence of organic sulphide compounds, Desalination 258 (2010) 206–218.

[46] Z. Aksu, Determination of the equilibrium, kinetic and thermodynamic parameters of the batch biosorption of nickel(II) ions onto *Chlorella vulgaris*, Process Biochemistry 38 (2002) 89–99.

[47] D. Park, Y.-S. Yun, J.Y. Kim, J.M. Park, How to study Cr(VI) biosorption: use of fermentation waste for detoxifying Cr(VI) in aqueous solution, Chemical Engineering Journal 136 (2008) 173–179.

[48] D. Mohan, C.U. Pittman Jr, Activated carbons and low cost adsorbents for remediation of tri- and hexavalent chromium from water, Journal of Hazardous Materials 137 (2006) 762–811.